



## Strengthening and Repairing of Reinforced Concrete Beams by Ferrocement

Prof. Yousry B I Shaheen<sup>1,\*</sup>, Dr. Noha M Soliman<sup>2</sup>, Eng. Afaf Rady El-Kashef<sup>3</sup>

<sup>1</sup>Civil Engineering Department, Faculty of Engineering, Menoufia University, Egypt

<sup>2</sup>Civil Engineering Department, Faculty of Engineering, Menoufia University, Egypt

<sup>3</sup>Civil Engineering Department, Faculty of Engineering, Menoufia University, Egypt

**Abstract:** This paper presents a proposed method for strengthening and repairing of reinforced concrete beams using ferrocement laminates as a viable alternative to steel plates and carbon fibers sheets which are directly glued to the cracked tension face of the beam by epoxy resins without shear connectors. The results of the experimental investigation to examine the effectiveness of this method are reported and discussed including strength, deflection, compressive and tensile strains, ductility ratio, Energy absorption properties and cracking characteristics of the strengthening and repairing of the reinforced concrete beams. Fifteen reinforced concrete beams were tested under four lines loadings until failure over simply supported 900mm span and having the dimensions of 50x100mm in cross section. The experimental program comprises three designations series. Series I include beam 1 control and beam 9 controls which conventional reinforced with steel bars and stirrups without and with polypropylene fibers respectively. Series II consists of beams 2-8 which were repaired after failure with various types of metallic and nonmetallic reinforcing materials. Series III comprises beams 10-15 which were strengthening with various layers of steel meshes while beam 15 was strengthening with one layer of tensor mesh. The experimental results of the repaired beams emphasized that irrespective of the type of used meshes expanded or welded steel mesh or the repair scheme, better cracking behavior for all test specimens could be achieved compared to their original behavior. Under short- term loading conditions, all repaired specimens restored more than their original ultimate strengths. The ductility ratio and energy absorption properties also improved by this proposed method of strengthening and repairing of beams by ferrocement.

**Keywords:** Ferro-cement; Beams with openings; Experimental program; Structural behavior; Analytical mode.

### الملخص العربي:

يقدم هذا البحث طريقة عملية مقترحة لتقوية وإصلاح الكمرات الخرسانية المسلحة باستخدام رقائق الفيروسيمنت كبديل لألواح الصلب وشرائح الألياف الكربونية المصقوفة بمواد إيبوكسية. وقد تم صب واختبار عدد 15 كمرة خرسانية مسلحة بالإضافة لعدد 7 كمرات والكمرات مستطيلة المقطع وبأبعاد 50مم عرض وبعق 100مم وبطول 1000مم تحت تأثير حمل الأنحاء (Four) lines loadings وبحر الكمرات ثابت 900مم وحتى حدوث الأنهييار وقد تم تسجيل الأحمال عند التشرخ الأول وعند حدوث الأنهييار وقياس الترخيم وقياس الأنفعال في كلا من منطقتي الشد والضغط وحساب نسبة الممتولية والطاقة المختزنة وحساب حمل التشغيل وتحديد أشكال التشرخات لجميع الكمرات المختبرة. وقد تم استخدام الشبك المعدني الملحوم والمجلفن والشبك المعدني الممدد وشبك التنصير وشبك البولي اثيلين وألياف البولي برويلين في أعمال تقوية وإصلاح الكمرات الخرسانية وتحليل النتائج العملية وعمل المقارنات اللازمة وقد توصل البحث الى زيادة أقصى حمل للكمرات المقواة بالطريقة المبتكرة بنسبة 63 و85%.

وتوصلت نتائج البحث الى أعلى نسبة زيادة أقصى حمل بالنسبة للكمرات التي تم اصلاحها بحوالي 68 و 123% بالإضافة الى زيادة نسبة الممتولية والطاقة المختزنة لجميع الكمرات الخرسانية ذات فائدة كبيرة في تحمل الأحمال الديناميكية والزلازل. والبحث عملي وتطبيقي يفيد العاملين في مجال الهندسة الإنشائية والتشييد ويوفر اقتصادى كبير للدول النامية والمتقدمة على السواء.

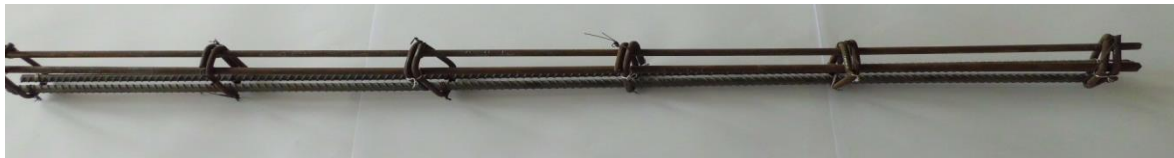
## 1. Introduction

Irons introduced laminated ferrocement as a new production technique of ferrocement. This technique has been used successfully for a wide variety of structural repairs and has proven to be impact and corrosion resistant. Water tanks and swimming pools could be renovated using an un-bounded ferrocement laminate on the interior surface while pressure vessels and tanks were reinforced by interior and external laminates containing high tensile wires between mesh layers Anwares et [1]. All presented a rehabilitation technique for reinforced concrete structural beam elements using ferrocement. This technique involved strengthening of reinforced concrete beams by the application of hexagonal chicken wire mesh and skeletal steel combined with ordinary plastering. Another study on using ferrocement as a structural repair material was presented by Paramasivan. Ong and Lim investigated the flexural behavior of reinforced concrete beams repaired with epoxy resin injection and strengthened using thin ferrocement laminates attached to the tension face of the damaged beams, [2, 3, 4, 5]. Ezzat Fahmy, Yousry Shaheen and Yasser Korany,[6,7,8] presented the results of both experimental and analytical investigation on the use of laminated ferrocement for strengthening and repairing damaged reinforced concrete beams due to overloading. The results showed that the repaired specimens reached the ultimate load which was more than that of the control specimens. Specimens loaded to collapse could be repaired with enhanced strength and reduced deflections. Yousry Shaheen et.al,[9] presented experimental results of strengthening and repairing of reinforced concrete beams with openings previously damaged by flexural loadings. The results emphasized superior strength gain with high ductility and energy absorption properties which are very useful for dynamic applications.

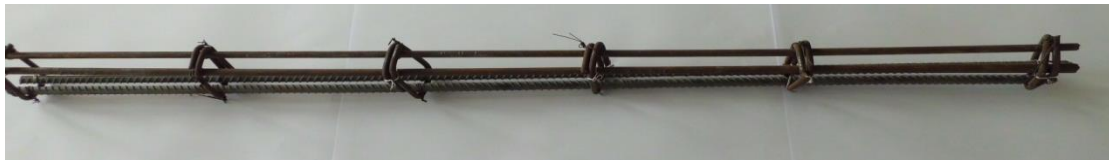
This paper presents the results of the experimental investigation to examine the effectiveness of this method are reported and discussed including strength, deflection, compressive and tensile strains, ductility ratio, Energy absorption properties and cracking characteristics of the strengthening and repairing of the reinforced concrete beams. Fifteen reinforced concrete beams were tested under four lines loadings until failure over simply supported 900mm span and having the dimensions of 50x100mm in cross section. The experimental program comprises three designations series. Series I include beam 1 control and beam 9 controls which conventional reinforced with steel bars and stirrups without and with polypropylene fibers respectively. Series II consists of beams 2-8 which were repaired after failure with various types of metallic and nonmetallic reinforcing materials. Series III comprises beams 10-15 which were strengthening with various layers of steel meshes while beam 15 was strengthening with one layer of tensor mesh. The experimental results of the repaired beams emphasized that irrespective of the type of used meshes expanded or welded steel mesh or the repair scheme, better cracking behavior for all test specimens could be achieved compared to their original behavior. Under short-term loading conditions, all repaired specimens restored more than their original ultimate strengths. The ductility ratio and energy absorption properties also improved by this proposed method of strengthening and repairing of beams by ferrocement.

## 2. Experimental Program and properties of used materials

The experimental program of this research was designed to investigate the feasibility and effectiveness of strengthening and repairing reinforced concrete beams. The type and number of the reinforcing steel mesh layers in the ferrocement laminate were investigated. To investigate the effect of these test parameters on the strength, stiffness, cracking behavior, ductility, and energy absorption properties of the tested strengthening and repairing beams. Two types of steel mesh reinforcement were employed. These types are welded galvanized wire mesh and expanded steel mesh. Single, double, three and four layers of each type were used. The experimental program comprised casting and testing of four series. Series I consists of two conventionally reinforced control beams 1 without fibers and beam 9 with fibers to study the effect of fibers on the structural behavior of reinforced concrete beams. All tested beams having the dimensions of 50mm width, 100mm depth and 1000mm length and all beams were tested under four lines loadings along span equal 900mm until failure. Series II comprises of test specimens 2, 3, 4, 5, 6, 7 and 8. Series III consists of test specimens 10, 11, 12, 13, 14 and 15. Series IV comprises repairing of beams 2,3,4,5,6,7,8. The details of the test specimens are given in Table 1 and the cross sections of the different designations are shown in Figures 1, 2, 3 and 4.

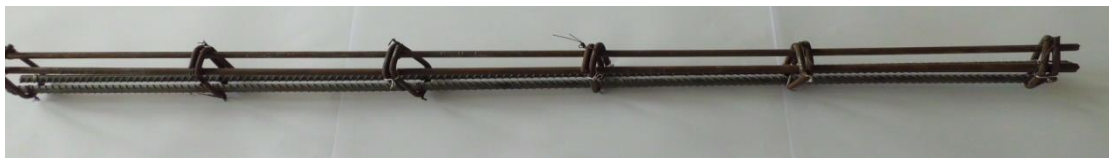


**Reinforcement of beam 1 control**



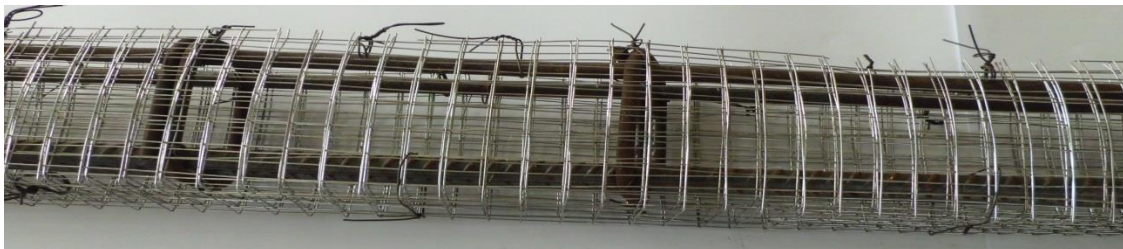
**Reinforcement of beam b9 control + polypropylene fibers**

**Fig. 1 Series I Control.**



**Reinforcement of beam b2-b8**

**Fig. 2 Series II**



**Reinforcement of beam b10 strengthened with 4 layers welded steel mesh**



**Reinforcement of beam b11 strengthened with 2 layers expanded steel mesh**



**Reinforcement of beam b12 strengthened with one-layer tensor mesh.**



**Reinforcement of beam b13 strengthened with one layer expanded steel mesh.**



**Reinforcement of beam b14 strengthened with two layers welded steel mesh.**



**Reinforcement of beam b15 strengthened with one layer polyethylene mesh.**

**Fig. 3 Series III**



Repairing of beam b2 by one layer expanded steel mesh at tension.



Repairing of beam b3 by two layers welded steel mesh at tension



Repairing of beam b4 by one layer U shape expanded steel mesh.



Repairing of beam b5 by four layers U shape welded steel mesh



Repairing of beam b6 by two layers U shape expanded steel mesh.



Repairing of beam b7 by two layers U shape welded steel mesh.



Repairing of beam b8 by one-layer U shape tensor mesh.

Fig. 4 Series IV Repairing of beams b2-b8

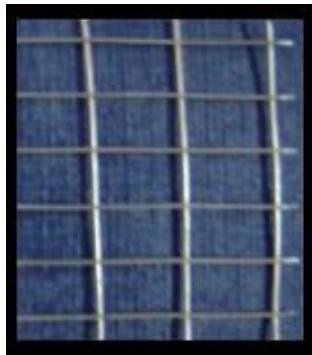
Table 1: Details of the Test Specimens

Group No.	Design. No. of Beams	Reinforcing Mesh			Reinforcing Steel Bars		
		Type	No. of layers	Volume Frac-tion %	Tens.	Comp.	Stirrups
<b>I cont.</b>	b1	----	-----	-----	2ø10	2ø8	6 ø6/m
	b9+fibers	----	-----	-----	2ø10	2ø8	6 ø6/m
<b>II</b>	b3	----	----	-----	2ø10	2ø8	6 ø6/m
	b4	----	-----	-----	2ø10	2ø8	6 ø6/m
	b5	-----	-----	-----	2ø10	2ø8	6 ø6/m
	b6	-----	-----	-----	2ø10	2ø8	6 ø6/m
	b7	-----	-----	-----	2ø10	2ø8	6 ø6/m
	b8	-----	-----	-----	2ø10	2ø8	6 ø6/m
<b>III Strength.</b>	b10	Welded U	4	1.096	2ø10	2ø8	6 ø6/m
	b11	expan. U	2	1.191	2ø10	2ø8	6 ø6/m
	b12	Tensar U	1	0.8	2ø10	2ø8	6 ø6/m
	b13	expan. U.	1	0.955	2ø10	2ø8	6 ø6/m
	b14	Welded U	2	0.548	2ø10	2ø8	6 ø6/m
	b15	Polyeth.. U	1	2.9	2ø10	2ø8	6 ø6/m
<b>IV repairing</b>	b2	expanded	1	0.191	2ø10	2ø8	6 ø6/m
	b3	welded	2	0.11	2ø10	2ø8	6 ø6/m
	b4	Exp. U	1	0.955	2ø10	2ø8	6 ø6/m
	b5	welded U	4	1.096	2ø10	2ø8	6 ø6/m
	b6	Exp. U	2	1.191	2ø10	2ø8	6 ø6/m
	b7	welded U	2	0.548	2ø10	2ø8	6 ø6/m
	b8	tensar U	1	0.8	2ø10	2ø8	6 ø6/m

### 2.1 Types of steel meshes used

Two types of steel meshes were used to reinforce the ferrocement beams. These types are expanded steel mesh and WSM welded steel mesh, Figure 5. The details of the geometric properties of these two types are given in Table 2.

Mesh type	Proof Stress (N/mm <sup>2</sup> )	Proof Strain x 10 <sup>-3</sup>	Ultimate Strength (N/mm <sup>2</sup> )	Ultimate Strain x 10 <sup>-3</sup>
-----------	--------------------------------------	---------------------------------	---	------------------------------------



a) Welded wire mesh



b) Expanded wire mesh



c) Tenser mesh



d) Polyethylene mesh



e) Polypropylene Fibers PP 300-e3



Types of Meshes and Fibers used.

Figure 5: Types of materials used.

Welded	737	1.17	834	58.8
Expanded	199	9.7	320	59.2

Table 2: Mechanical properties of steel meshes\

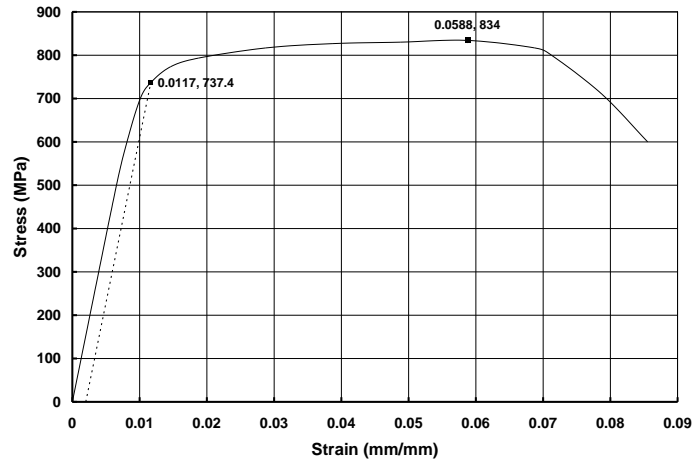


Figure 6: Stress-strain relationship for the welded wire mesh

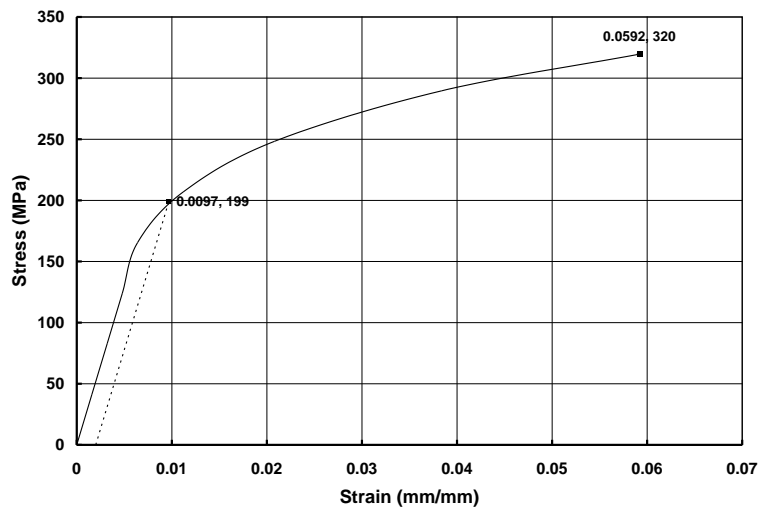


Figure 7: Stress-strain relationship for the expanded steel mesh

## 2.2 Concrete and Mortar Mixes

### 2.2.1 Concrete Mix

Concrete was used for the control specimens and for the core of the beams of the designations with conventional concrete core. For the concrete used throughout this research, the cement content used was  $330 \text{ kg/m}^3$ . Water-cement ratio was kept constant at value of 0.4; this value was chosen after many trial- mixes based on ACI 211.1-81 for cube strength,  $f_{cu}$ , of 35 MPa.

### 3. Preparation of Test Specimens

A wooden mold has been utilized to cast ferrocement rectangular sections shaped forms. The wooden mold consists of three events to produce three beams having the dimensions of 50mm with, 100 height and 1000mm long at the same time as shown in Figure 8.



**Fig. 8 Wooden mold for casting beams.**

#### 3.1 Test setup

After 28 days, the specimens were painted with white paint for better crack detection and marking during the testing process. A set of three dial gauges were placed under the test specimen to measure the deflections at three locations. All test specimens were tested on the universal testing machine. The test was conducted under four line loadings as shown in Figure 9. The specimen was centered on the testing machine, where the span between the two supports was kept at 1400mm. A dial gauge was placed under the center of the specimen to measure the deflection versus load. The load was applied at 5 KN increments, by a hydraulic jack, on. Cracks were traced and marked throughout the side of the specimen. The first crack-load of each specimen, crack propagation, and failure mode was recorded. The load was increased until the failure of the specimen.



**Fig. 9 Test set up**

### 4. Experimental Results and Discussions

## 4.1 Introduction

The experimental results of the test program and the discussions are presented in this chapter. Comparisons are conducted between the results of the different test groups to examine the effect of type of steel reinforcement, the volume fraction of provided steel reinforcement. The effects of these parameters on the structural responses of the proposed beams in terms of failure load, mode of failure, first crack load, serviceability load, ductility ratio, and energy absorption were studied.

The results of all test specimens are listed in Table 3. Figures 10-24 Show the load central deflection curves for all test specimens measured at the center and of all beams, while Figs. 16-22 show the central deflections for all the tested repaired beams, B2, B3, B4, B5, B6, B7 and B8 respectively. Table 3 shows the obtained experimental results for each specimen. The table shows the obtained results for the first crack load, serviceability load, ultimate load, deflection at ultimate load, ductility ratio, and energy absorption. Ultimate load and deflection at ultimate load were measured and obtained during the test, while the first crack load, service load, ductility ratio and energy absorption were determined from the load-deflection diagram for each specimen. The first crack load was determined from the load-deflection curve at the point at which the load-deflection curve started to deviate from the linear relationship. The Service load, or flexural serviceability load, is defined in this investigation as the load corresponding to deflection equal  $\text{Span}/250$ .

## 4.2 Behavior of the Test Specimens

The Behavior of the conventional reinforced concrete and that reinforced with closely spaced wire steel mesh differs because of the uniformity of reinforcement distribution along the section, geometry of reinforcement, type of reinforcement, specific surface area, a volume fraction of reinforcement, and mortar cover. These parameters have effects on the serviceability load and deflection control, cracking behavior, ultimate strength, ductility ratio, and energy absorption properties.

### 4.2.1 Deformation Characteristics

The plotted central deflections of the test specimens against the applied load are shown in Figures 10-24 and Figs. 25-31. It can be seen from these Figures that the load-deflection relationship of the test specimens can be divided into three stages as follows:

- a) Elastic behavior until the first cracking. The load-deflection relationship in this stage is linear. The slope of the load-deflection curve in this stage varies with different types of the test specimens. The end of this stage is marked by the deviation from linearity. The extent of this stage vary with the type and number of layers of the steel meshes.
- b) In the second stage, the slope of the load-deflection curve changes gradually due to the expected reduction in the specimens' stiffness as the result of multiple cracking. The gradient of the load-deflection curve increases with the increase of the volume fraction of the reinforcement.
- c) In the third stage, large plastic deformation occurred as the result of yielding of the reinforcing bars and the steel meshes in the ferrocement beams. The load-deflection relationship for the control specimens was linear up to a first crack load after which the relation became nonlinear.

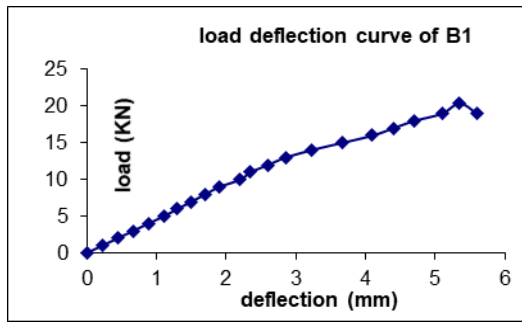


**Fig. 10** Load deflection curves of beam B1

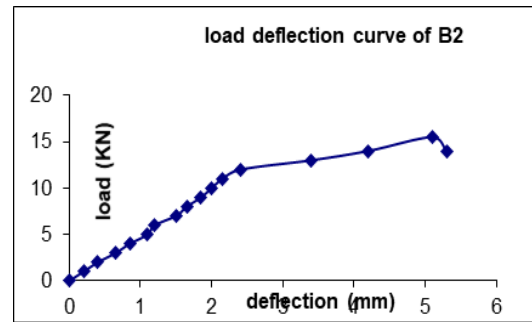


**Fig. 11** Load deflection curves of beam B2

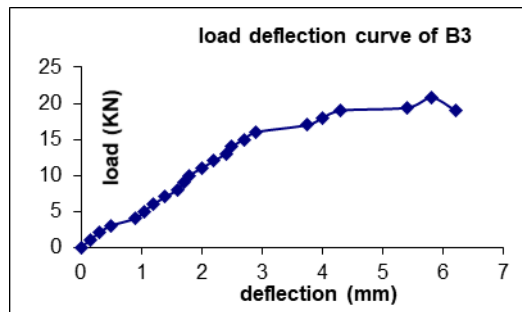


**Fig. 12** Load deflection curves of beam B3

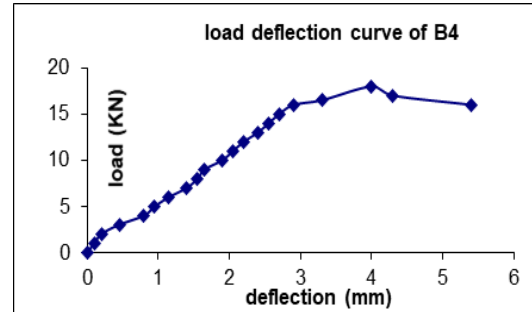


**Fig. 13** Load deflection curves of beam B4

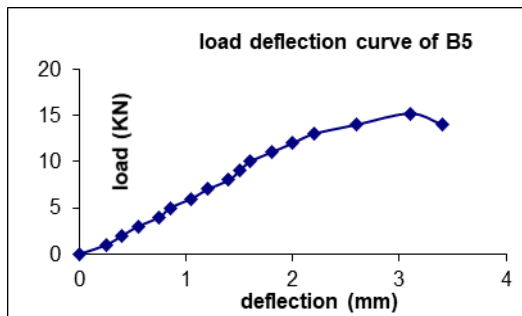


**Fig. 14** Load deflection curves of beam B5

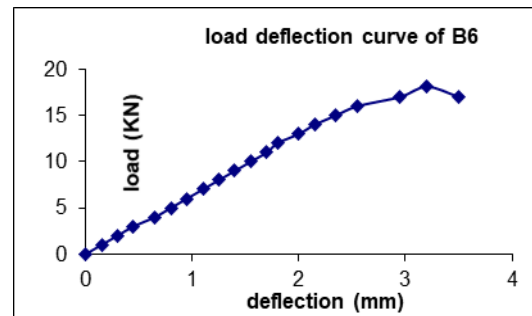


**Fig. 15** Load deflection curves of beam B6

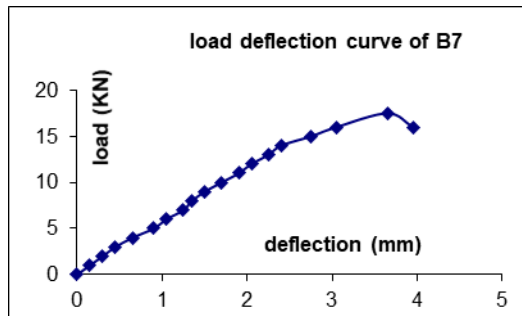


**Fig. 16** Load deflection curves of beam B7

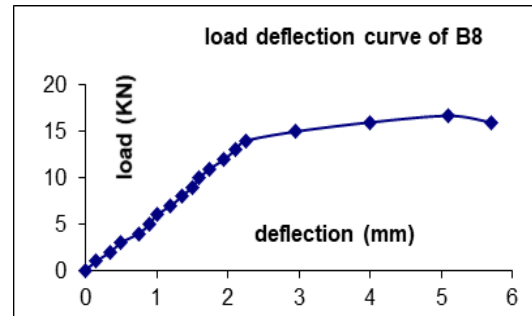


**Fig. 17** Load deflection curves of beam B8

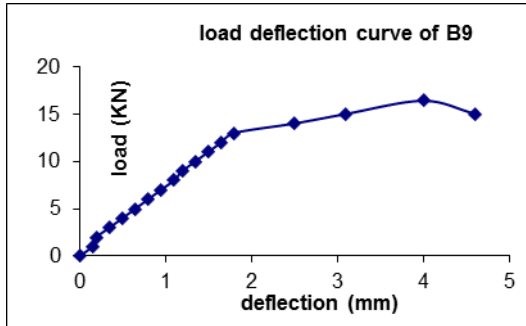


Fig. 18 Load deflection curves of beam B9

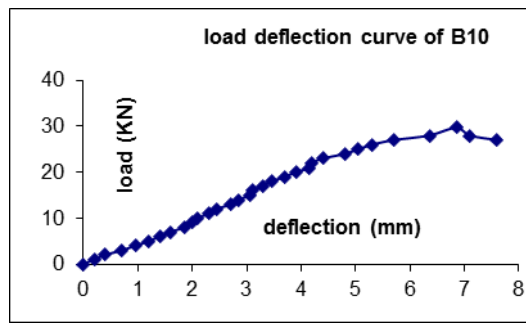


Fig. 19 Load deflection curves of beam B10

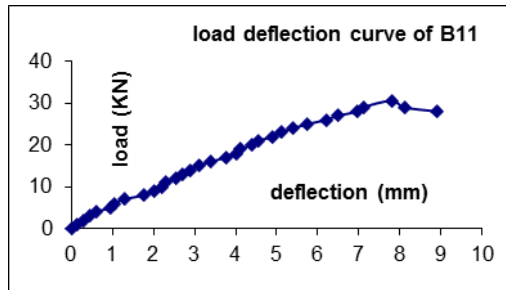


Fig. 20 Load deflection curves of beam B11

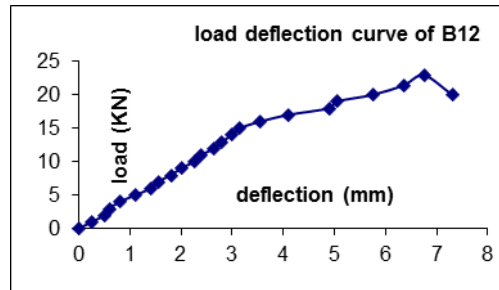


Fig. 21 Load deflection curves of beam B12

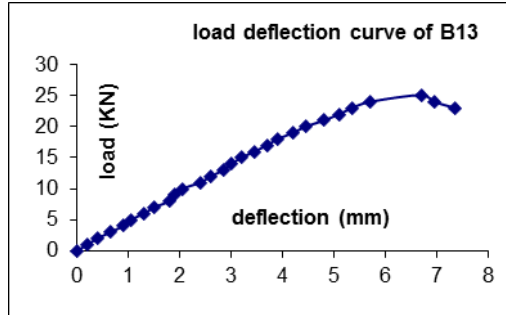


Fig. 22 Load deflection curves of beam B13

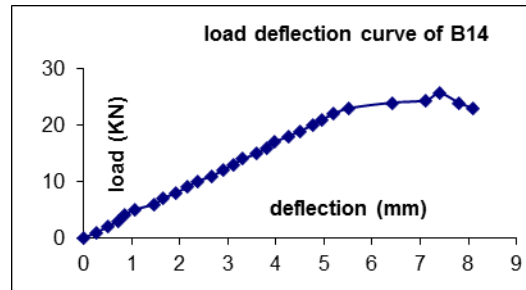


Fig. 23 Load deflection curves of beam B14

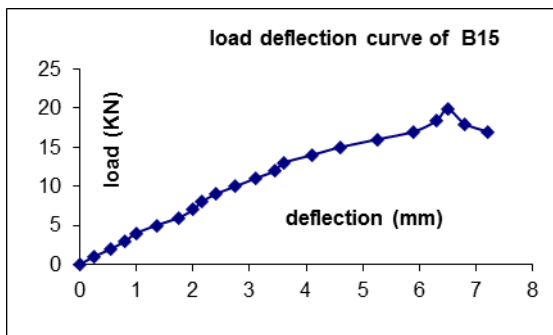


Fig. 24 Load deflection curves of beam B15

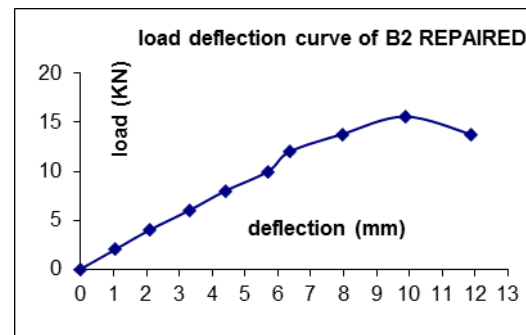
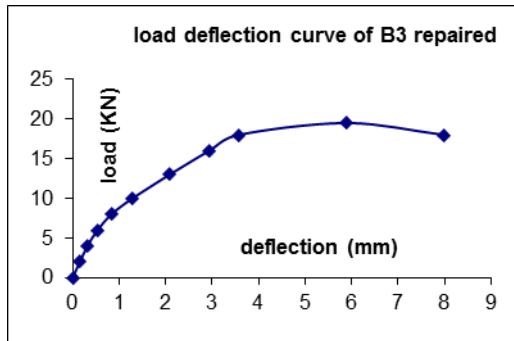
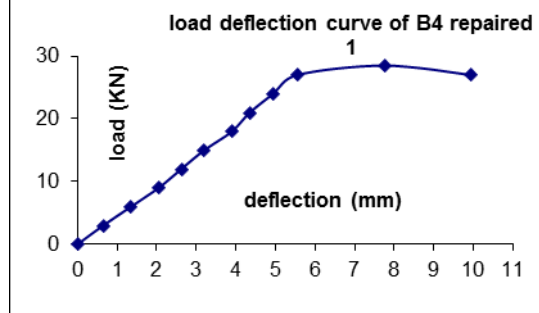


Fig. 25 Load deflection curves of beam B2 repaired



**Fig. 26** Load deflection curves of beam B3 repaired



**Fig. 27** Load deflection curves of beam B4 repaired

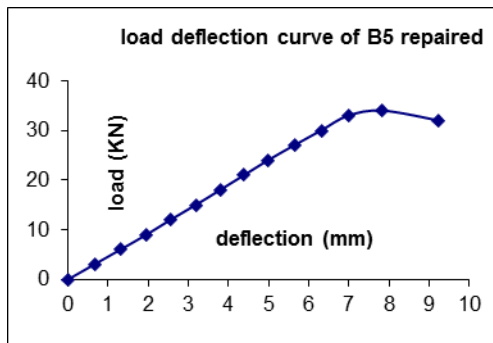


**Fig. 28** Load deflection curves of beam B5 repaired

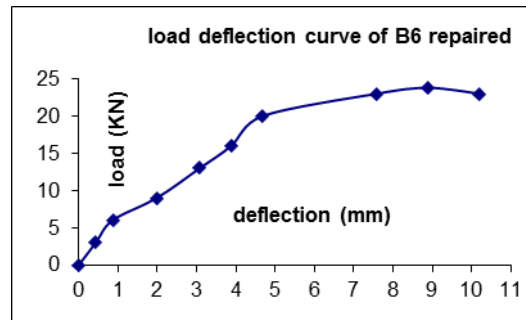


**Fig. 29** Load deflection curves of beam B6 repaired

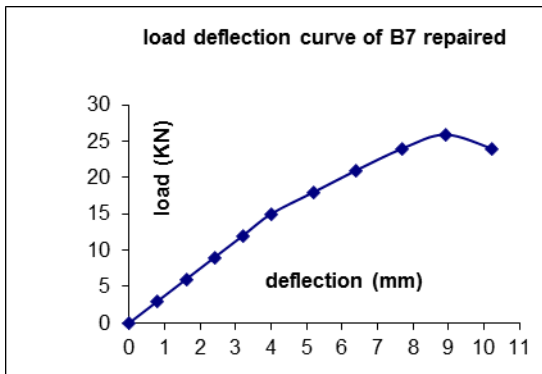


**Fig. 30** Load deflection curves of beam B7 repaired

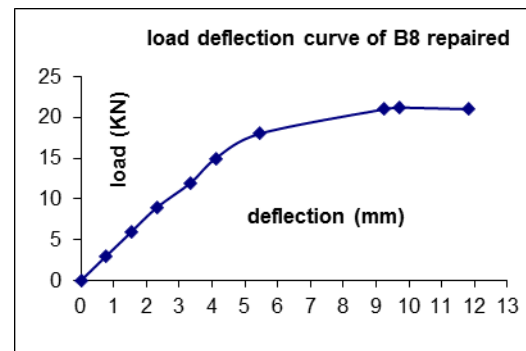


**Fig. 31** Load deflection curves of beam B8 repaired

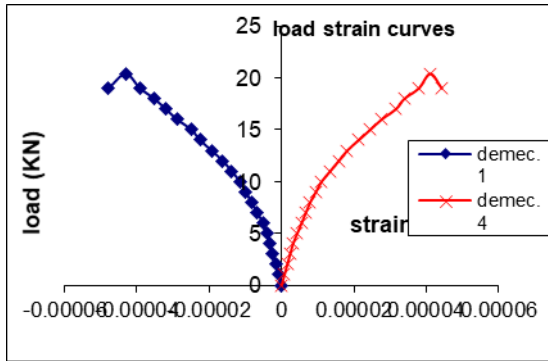


**Fig. 32 Load strain curves of beam B1.**

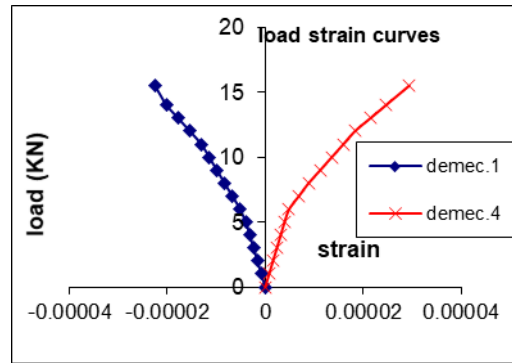


**Fig. 33 Load strain curves of beam B2.**

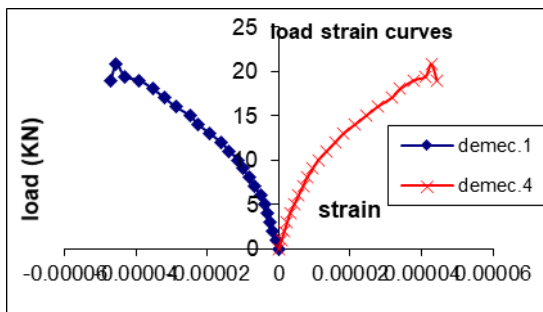


**Fig. 34 Load strain curves of beam B3**

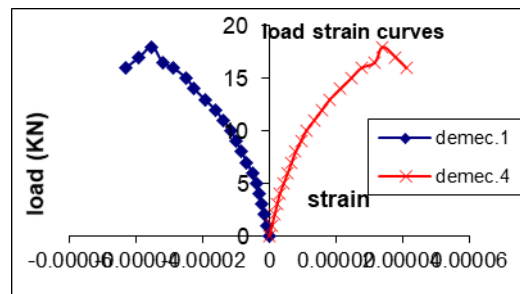


**Fig. 35 Load strain curves of beam B4**

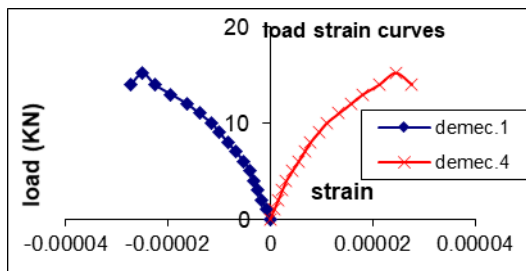


**Fig. 36 Load strain curves of beam B5**

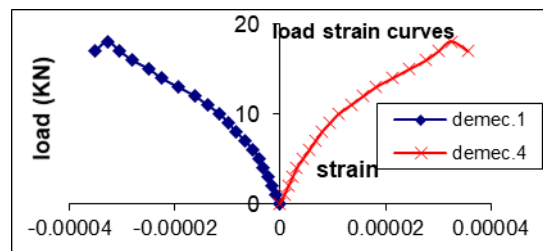


**Fig. 37 Load strain curves of beam B6**

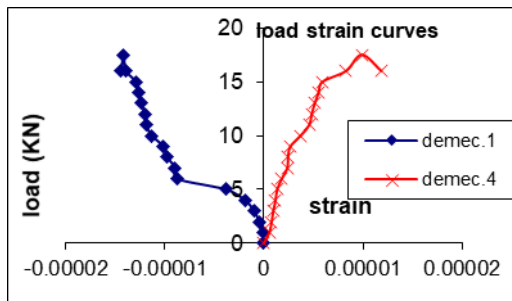


**Fig. 38 Load strain curves of beam B7**

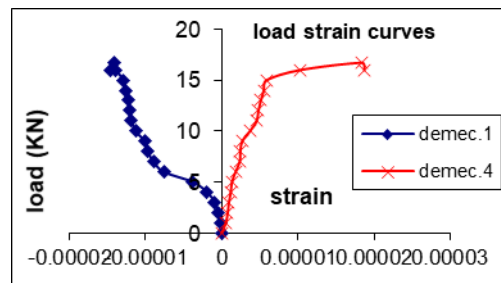


**Fig. 39 Load strain curves of beam B8**

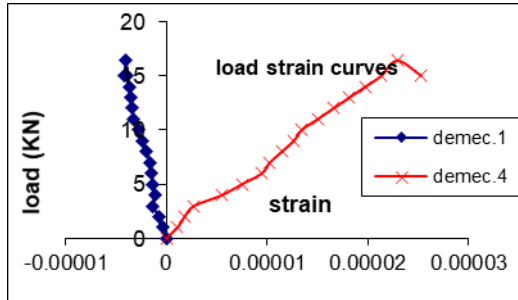


**Fig. 40 Load strain curves of beam B9**

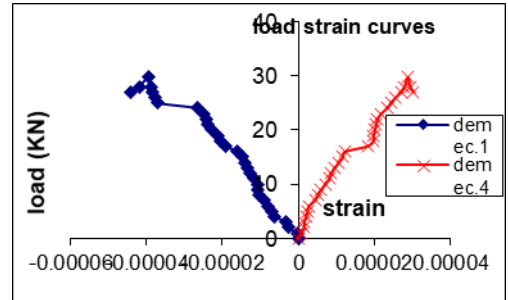


**Fig. 41 Load strain curves of beam B10**

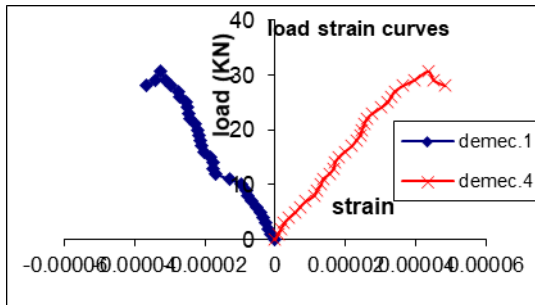


**Fig. 42 Load strain curves of beam B11**

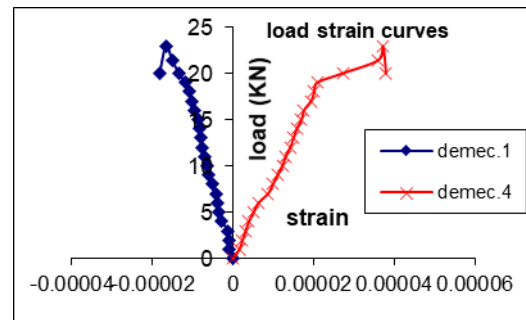


**Fig. 43 Load strain curves of beam B12**

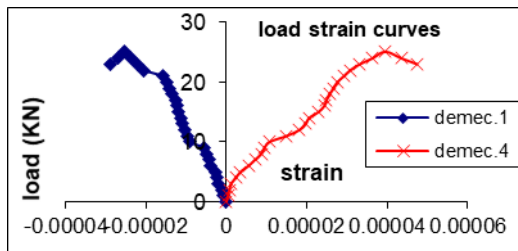


**Fig. 44 Load strain curves of beam B13**

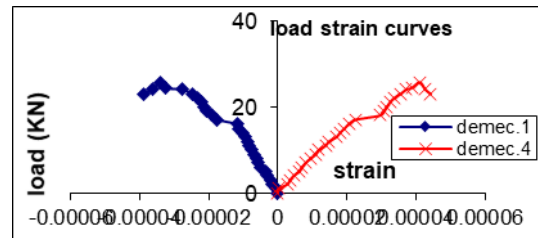


**Fig. 45 Load strain curves of beam B14**

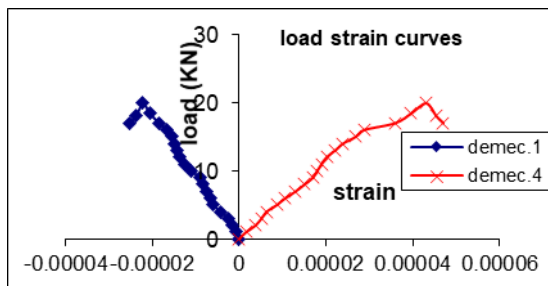


**Fig. 46 Load strain curves of beam B15**

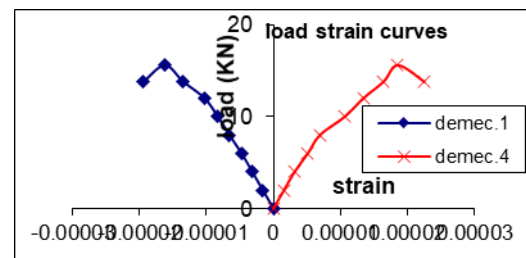


**Fig. 47 Load strain curves of beam B2 repaired**

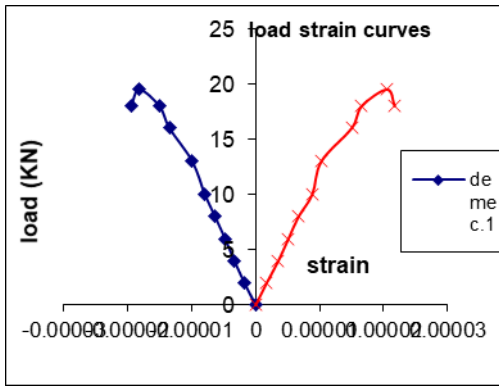


**Fig. 48 Load strain curves of beam B3 repaired**

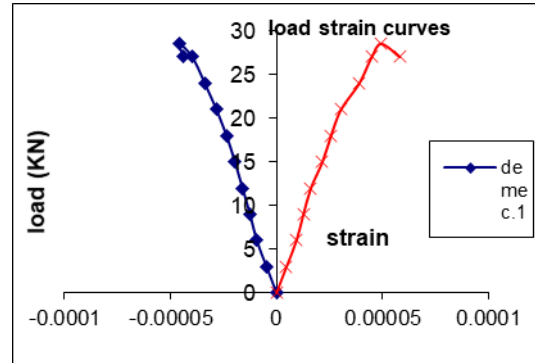


**Fig.49 Load strain curves of beam B4 repaired**

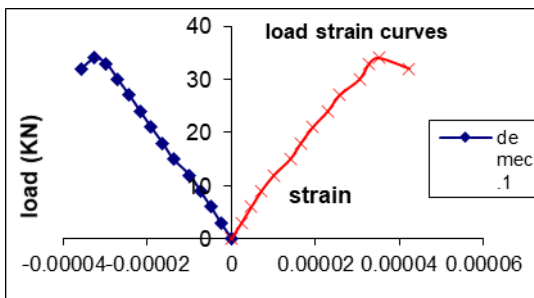


**Fig.50 Load strain curves of beam B5 repaired**

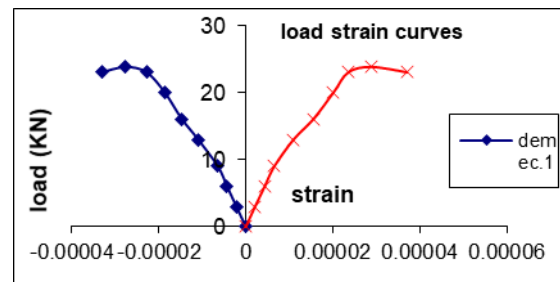


**Fig.51 Load strain curves of beam B6 repaired**

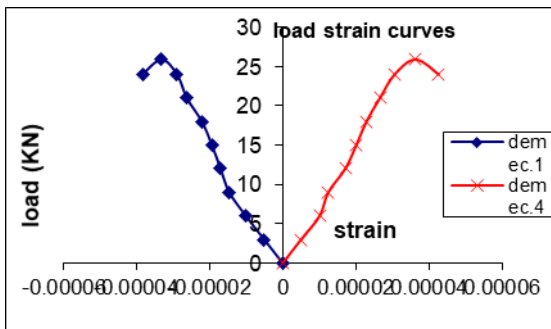


**Fig.52 Load strain curves of beam B7 repaired**

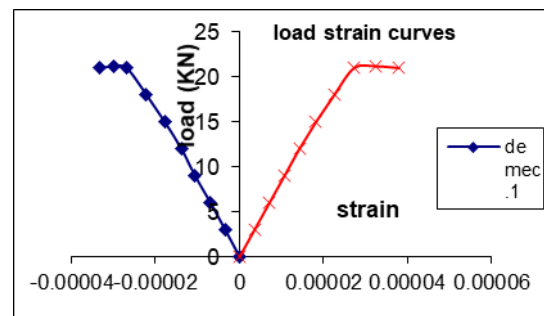


**Fig.53 Load strain curves of beam B8 repaired**

#### 4.2.2 Concrete strains

Figs. 32- 46 show load tensile and compressive strains curves of all the tested beams respectively. Table 3 presented maximum tensile and compressive strains of all the tested beams. Figs. 47-54 show load tensile and compressive strains curves of all repaired beams B2-B8 respectively.

**Table 3: Maximum tensile and compressive strains of all tested beams.**

Beam designation	Maximum Load, KN	Tensile strain	Compressive strain
B1	20.4	0.0000416	0.0000431
B2	18.5	0.00002939	0.00022575
B3	20.8	0.00004266	0.0000454
B4	18.0	0.00003397	0.000035755
B5	15.2	0.00002449	0.00002488
B6	18.1	0.00003239	0.00003278
B7	17.5	0.000009875	0.00001414
B8	16.7	0.0000184	0.0001414
B9	16.4	0.00002291	0.00003995
B10	29.7	0.0000288	0.0000395
B11	B11	0.00004345	0.00003278
B12	22.9	0.00003713	0.00001659
B13	25.1	0.0000395	0.00002528
B14	25.7	0.00004108	0.00003397
B15	19.9	0.000043053	0.00002212

**Table 4 Maximum tensile and compressive strains of all repaired tested beams.**

Beam designation	Maximum Load, KN	Tensile strain	Compressive strain
B2	15.6	0.00001856	0.000016195
B3	19.5	0.00002054	0.00001817
B4	28.5	0.000049375	0.00004574
B5	34.0	0.000035155	0.000033255
B6	23.8	0.000028756	0.0000274
B7	25.9	0.00003534	0.00003318
B8	21.2	0.000003239	0.00003002



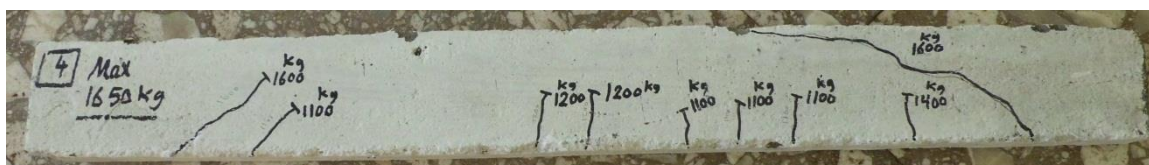
**Fig. 54 Cracking pattern of beam 1C.**



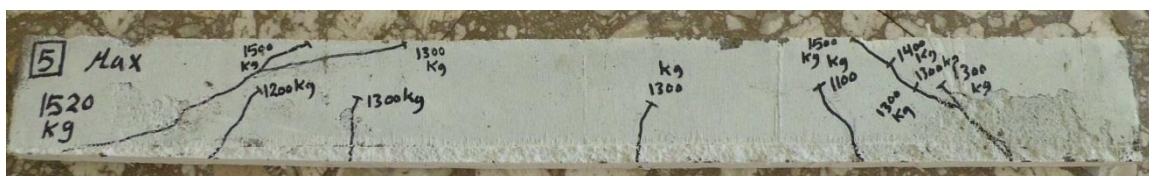
**Fig. 55 Cracking pattern of beam 2.**



**Fig. 56 Cracking pattern of beam 3.**



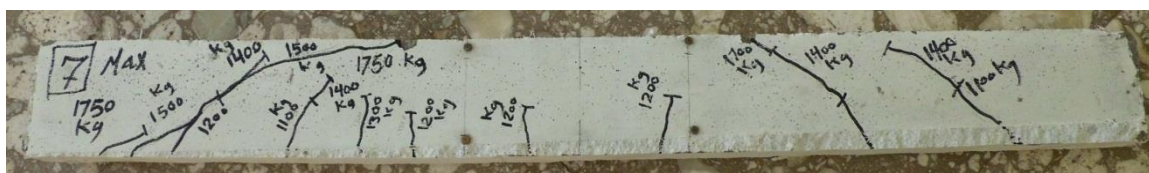
**Fig. 57 Cracking pattern of beam 4.**



**Fig. 58 Cracking pattern of beam 5.**



**Fig. 59 Cracking pattern of beam 6.**





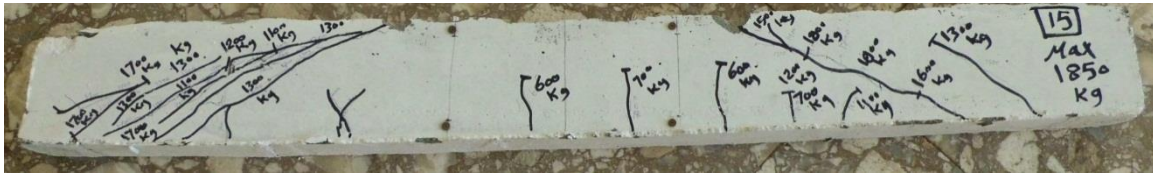


**Fig. 68 Cracking pattern of beam 15.**



**Fig. 69 Cracking pattern of beam 2 Repaired.**



**Fig. 70 Cracking pattern of beam 3 Repaired.**



**Fig. 71 Cracking pattern of beam 4 Repaired.**



**Fig. 72 Cracking pattern of beam 5 Repaired.**

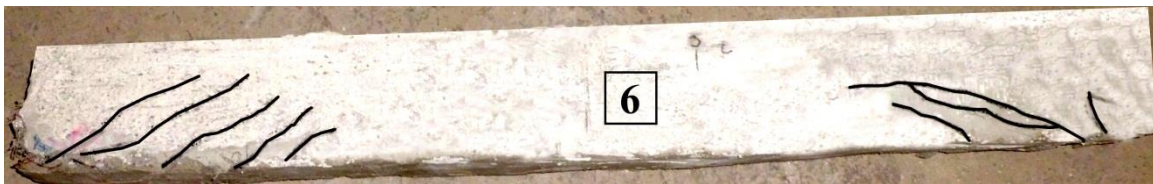


**Fig. 73 Cracking pattern of beam 6 Repaired.**



**Fig. 74 Cracking pattern of beam 7 Repaired.**

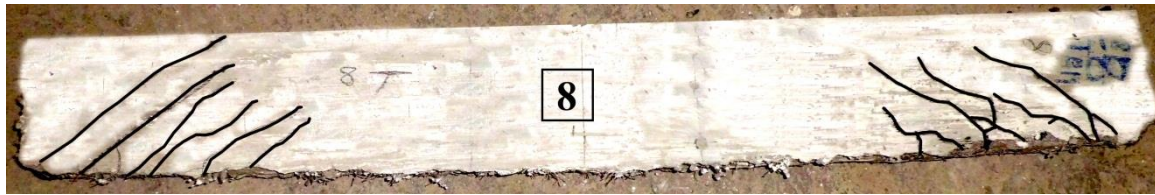
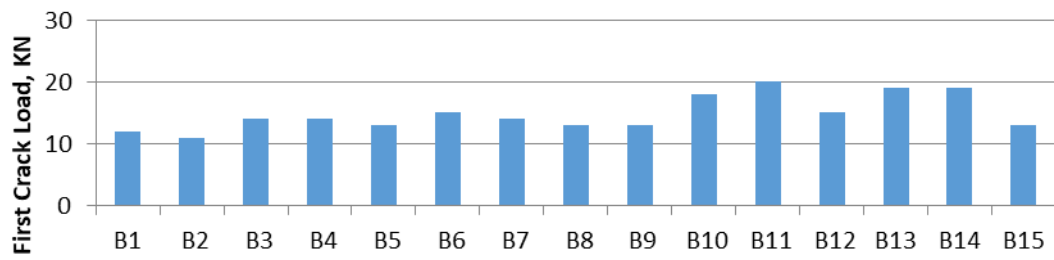


**Fig. 75 Cracking pattern of beam 8 Repaired.**

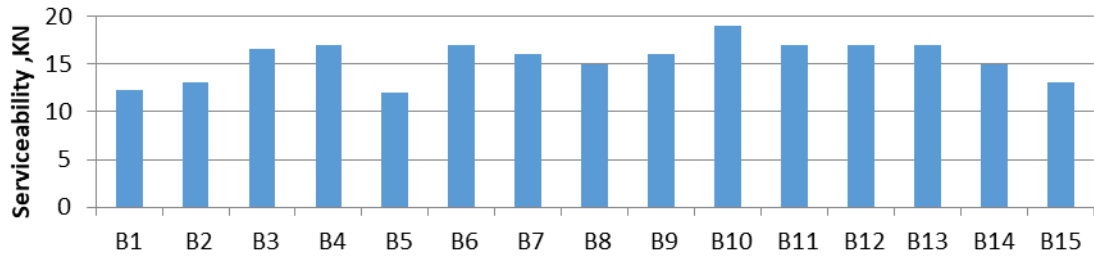
**Table 5: First crack, ultimate, serviceability loads, and ductility ratio and energy absorption properties for tested beams.**

Beam designation	F.C.,KN	P.serv. KN	P.ult., KN	def.F.C., mm	max.def, mm	Ductility ratio	Energy ab- sorption KN/mm
<b>B1</b>	12	12.3	20.4	2.6	3.35	1.29	64.42
<b>B2</b>	11	13	15.5	2.15	3.3	1.53	53.375
<b>B3</b>	14	16.5	20.8	2.5	6.2	2.48	84.37
<b>B4</b>	14	17	18	2.55	5.4	2.12	65.37
<b>B5</b>	13	12	15.2	2.2	3.4	1.55	31.23
<b>B6</b>	15	17	18.1	2.35	3.5	1.49	37.31
<b>B7</b>	14	16	17.5	2.4	3.95	1.65	41.7
<b>B8</b>	13	15	16.7	2.1	5.7	2.72	69.21
<b>B9</b>	13	16	16.4	1.8	4.6	2.56	53.8
<b>B10</b>	18	19	29.7	3.45	7.6	2.20	132.21
<b>B11</b>	20	17	30.6	4.4	8.9	2.02	166.65
<b>B12</b>	15	17	22.9	3.15	7.3	2.326	101.35
<b>B13</b>	19	17	25.1	4.2	7.35	1.75	97.9
<b>B14</b>	19	15	25.7	4.5	8.1	1.8	126.55
<b>B15</b>	13	13	19.9	3.6	7.2	2	81.83

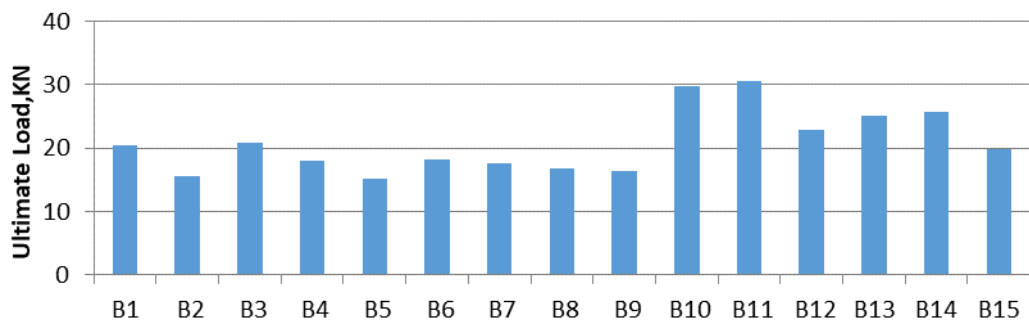
**Fig. 76 First Crack of tested Beams.**



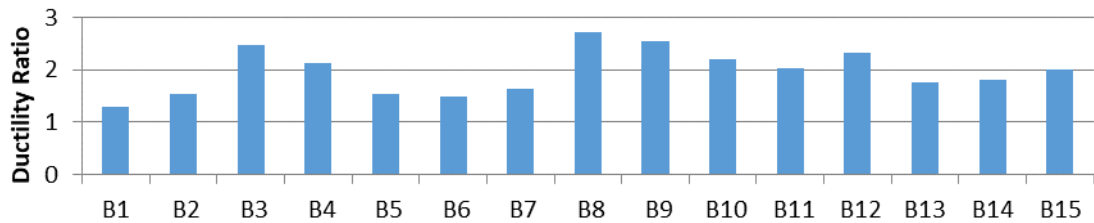
**Fig. 77 Serviceability Load of Tested Beams.**

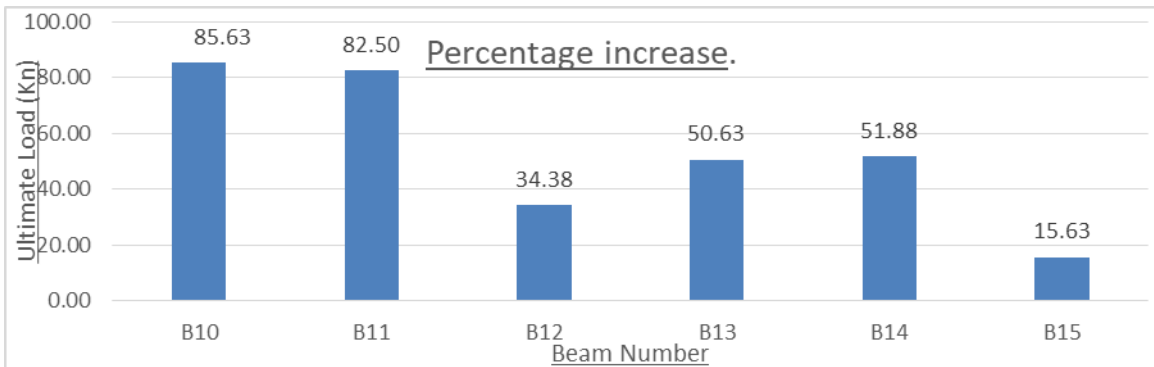
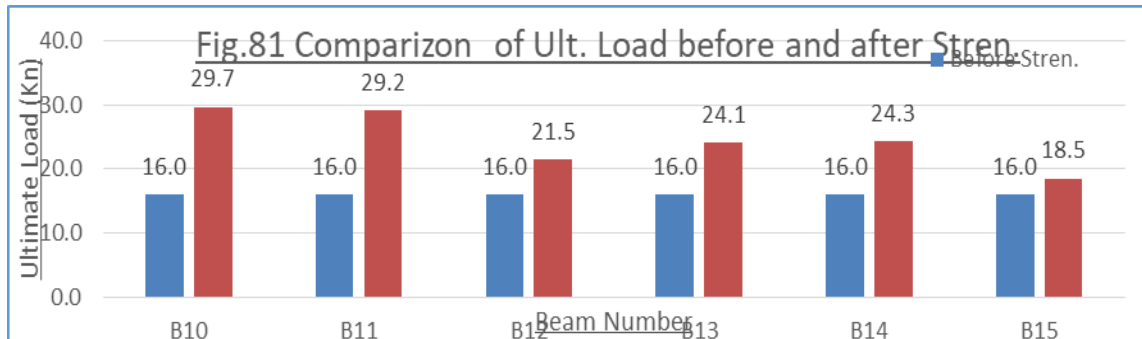
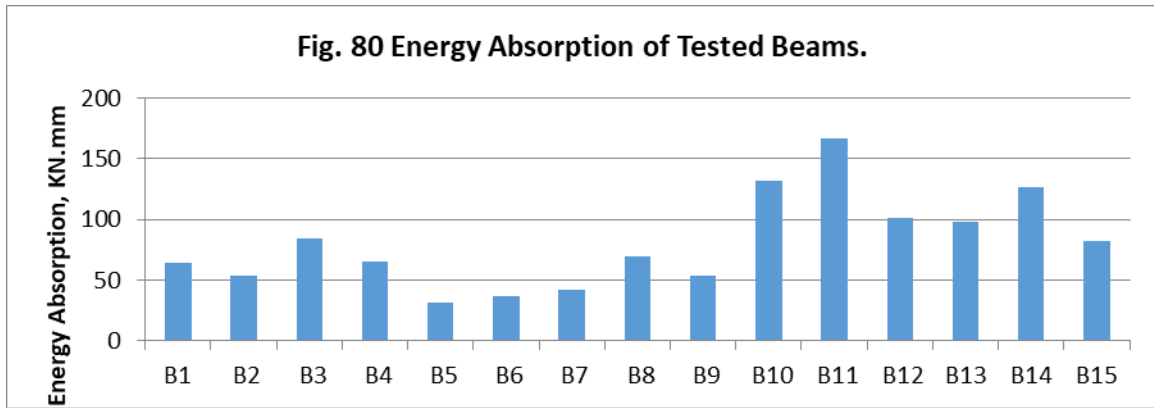


**Fig. 78 Ultimate Load of Tested Beams.**

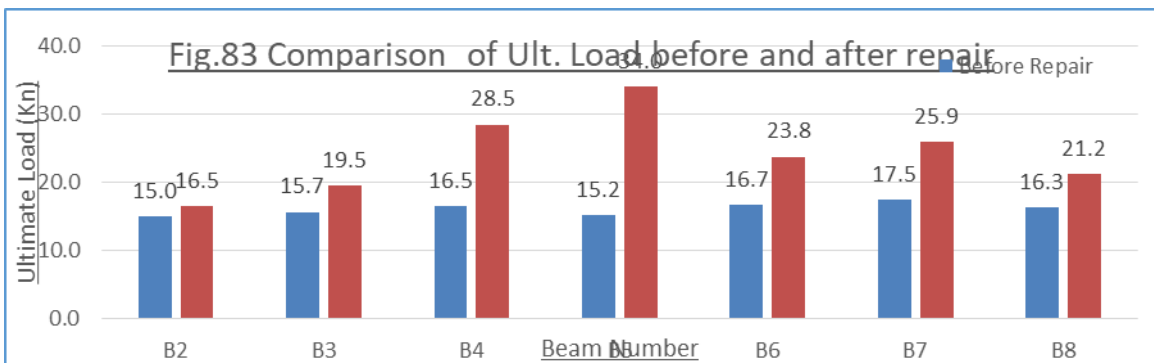


**Fig. 79 Ductility Ratio of Tested Beams.**





**Fig.82 Percentage increase in ultimate loads of Beams B10-b15**



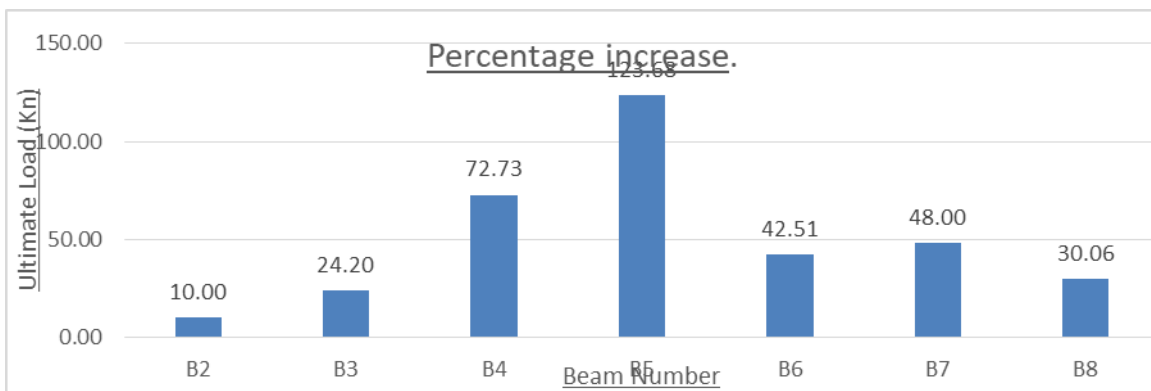


**Fig.84 Percentage increase in ultimate loads of Beams B2-B8.**

### 4.3 Cracking Behavior

Cracking is one of the most important phenomena that help to assess the behavior of concrete elements, failure mechanism, and mechanical properties. In this section crack pattern and failure modes are described and discussed. In general, no shear failure occurred in any of groups. It is clear that the existence of the ferrocement forms had a major effect on the cracking patterns and failure mechanisms. It is worth mentioning that no sound of mesh fracture was heard at failure of all the test specimens.

For the control specimens, 1C, cracks started at the mid-span at the bottom edge of the beam. Upon increasing the load, the cracks propagated rapidly upwards and increased in number along with the span. The length and width of the cracks increased with the increase of the applied load. Moreover, diagonal or inclined cracks developed at both ends of the specimen. It is worth mentioning that before failure, spalling of the concrete cover was observed. Failure of the control specimens occurred due to the crushing of the concrete surface as shown in Figure 54

Figures 55-68 show the cracking patterns for test B2-B15 respectively. While Figures 69- 75 show cracking patterns of repaired beams B2- B8 respectively. It is interesting to note that specimens of the group repaired with various layers of Welded steel mesh exercise better-cracking patterns. The first crack for this group occurred nearly at mid-span. As the load increased, it was noticed that new cracks were developed at both sides of the first crack, while the first crack propagated vertically. With the additional increase of the load, new parallel cracks were developed while the previously developed cracks propagated nearly vertically. This pattern of cracks development continued till failure of beams. There is no spalling of concrete cover this is predominant.

The crack patterns of test specimens of the group repaired with various layers of expanded steel mesh were similar to those of the previous group reinforced with welded layers of steel mesh. The first crack occurred nearly at mid-span. As the load increased, it was noticed that new parallel cracks were developed at both sides of the first crack, while the first crack propagated vertically. With the additional increase of the load new vertical cracks were developed, while the previously developed cracks propagated upwards. There are no signs of shear failure were observed for this group as shown in Figs. 69-75.

### 4.4 Structural behavior

#### 4.4.1 First crack load

Fig 76 shows the comparison of the first crack loads of all the tested beams. It is interesting to note

that beam B11 emphasizes the heights first crack load reached 20 KN.

#### **4.4.2 Serviceability load**

Fig. 77 shows the comparison of the serviceability loads of all the tested beams. It is interesting to note that beam B10 emphasizes the heights serviceability load reached 19 KN.

#### **4.4.3 Ultimate load**

Fig. 78 shows the comparison of the ultimate loads of all the tested beams. It is interesting to note that beam B11 emphasizes the heights ultimate load reached 30.6 KN.

#### **4.4.4 Ductility ratio**

Ductility ratio is defined here as the ratio of the deflection at ultimate load to that at first crack load. Fig. 79 shows the comparison of the ductility ratios of all the tested beams. It is interesting to note that beam B8 emphasizes the heights ductility ratio reached to 2.72.

#### **4.4.5 Energy absorption**

Energy absorption is defined here as the total area under load-deflection curves of all the test specimens. Fig. 80 shows the comparison of energy absorption of all the tested beams. It is interesting to note that beam B11 emphasizes the heights energy absorption reached to 166.65 KN.mm. The obtained values of both ductility ratios and energy absorption are very useful for dynamic applications.

#### **4.4.6 Comparison of Ult. Load before and after Strengthening**

Fig. 81 shows the comparison of ultimate loads of beams B10-B15 before and after strengthening of all the tested beams. It is interesting to note that beam B10 emphasizes the heights ultimate load reached 29.7 KN. Fig. 82 shows the comparison of percentage increase of ultimate load reached 85.63% that is great.

#### **4.4.7 Comparison of Ult. Load before and after repairing**

Fig. 83 shows the comparison of ultimate loads of beams B2-B8 before and after repairing of all the tested beams. It is interesting to note that beam B5 emphasizes the heights ultimate load reached 34 KN. Fig. 84 shows the comparison of percentage increase of ultimate load reached 123.68 % that is so great.

## **5.2 Conclusions**

Based on the results and observations of the experimental investigation presented regarding the effectiveness of laminated ferrocement in repairing reinforced concrete beams, the following conclusions could be drawn as follows:

1. Under short time loading conditions, reinforced concrete beams failed due to overloading can be restored with enhanced strength and performance using laminates, provided that they are suitably repaired and shear connectors are adequately spaced to ensure composite action until failure.
2. After repairing all test specimens emphasized large deflection at ultimate load, a significant increase in ductility ratio, and a considerable increase in the energy absorption as well. High ductility and energy absorption properties are very important characteristics, especially for dynamic loading applications.

3. Irrespective of the type of mesh used, repairing concrete beams with a U-shaped layer around the beam cross-section increased the gain in the ultimate moment about three times that obtained when only one laminate attached to the tension face was employed. Also, the U-shaped layer resulted in about double the increase in the energy absorption obtained using one layer, yet it gave a relatively lower increase in the ductility ratio.
4. The steel ratio used in the repair layer has a great influence on the amount of gain in a resisting moment ( $M_u$ ), the ductility ratio, and energy absorption. The higher; the steel ratio; the higher gain in ( $M_u$ ) and energy absorption, conversely, the ductility ratio was found to be decreased with the increase in the volume fraction percentage of reinforcing materials.

## References

- [1] Anwar A. W.; Nimityongskul, P.; Pama, R.P.; and Robles. Austriaco, L. , 1991. Method of rehabilitation of dtructural beam elewments using ferrocement, *Journal of Ferrocement* 21(3):P 229-254.
- [2] Lee, P. Paramasivam, C. T. Tam, K. C. G. Ong, and K. H. Tan (1990) "Ferrocement Alternative Material for Secondary Roofing Elements," *ACI Materials Journal*, Title No. 87-M41, pp.378-386.
- [3] Paramasivam, P., Ong, K. C. G. and Lim, C. T. E. (1994) "Ferrocement laminates for Strengthening RC T-Beams" *Cement and Concrete Composites*, Vol. 16, pp. 143-152.
- [4] Paramasivam, P and Sri Ravindrarajan, R. (1988) "Effect of Arrangements of Reinforcements on Mechanical Properties of Ferrocement, *ACI Structural Journal*, pp.3-11
- [5] Paramasivam, P., Ong, K., and Lim, C. 19993. Repair of damaged R.C. beams using ferrocement laminates. In *Proceedings of the fourth International Conference on Structural Failure*, 613-620.
- [6] Fahmy, E.H., Shaheen, Y.B., and Abou Zeid, M. N. (2004) "Development of Ferrocement Panels for Floor and Wall Construction", 5th Structural Specialty Conference of the Canadian Society for Civil Engineering, pp. ST218-1-ST218-10.
- [7] Fahmy, E.H., Shaheen, Y.B.I., and Korany, Y.S., April (1999) "Repairing Reinforced Concrete Columns Using Ferrocement Laminates", *Journal of Ferrocement*: Vol. 29, No. 2, pp. 115-124.
- [8] Fahmy, E.H., Shaheen, Y.B.I., and Korany, Y.S., January (1997) "Repairing Reinforced Concrete Beams b Ferrocement", *Journal of Ferrocement*: Vol. 27, No. 1, pp. 19-32
- [9] Yousry B.I. Shaheen, Noha M. Soliman, Eng. Fathya El-Araby "Repairing Reinforced Concrete Beams with Opening by Ferrocement Laminates" 12<sup>th</sup> International Conference on Civil and Architecture Engineering ICCAE-12-2018, April 3-5, 2018, *Military Technical College, Cairo, Egypt*.